# Supporting Information

# Paip2A inhibits translation by competitively binding to the RNA recognition motifs of PABPC1 and promoting its dissociation from the poly(A) tail

Takeru Sagae[1], Mariko Yokogawa[1], Ryoichi Sawazaki[1], Yuichiro Ishii[1], Nao Hosoda[2], Shin-ichi Hoshino[2], Shunsuke Imai[3, 4], Ichio Shimada[3, 4], Masanori Osawa*[1]

[1] Graduate School of Pharmaceutical Sciences, Keio University, Shibakoen, Minato-ku, Tokyo 105-8512, Japan

[2] Graduate School of Pharmaceutical Sciences, Nagoya City University, Tanabe-dori, Mizuho-ku, Nagoya 467-8603, Japan

[3] Graduate School of Pharmaceutical Sciences, The University of Tokyo, Hongo, Bunkyo-ku, Tokyo 113-0033, Japan

[4] Center for Biosystems Dynamics Research, RIKEN, Suehiro-cho, Tsurumi-ku, Yokohama 230-0045, Japan

* Correspondence should be addressed to M.O. (osawa-ms@pha.keio.ac.jp)

## Materials
- Supporting text
- Supporting Figure S1–S19
- Supporting Table S1, S2

# Supporting text

## Comparison of spectra of RRM2/3, RRM2, and RRM3

Overlay of the $^1$H-$^{15}$N HSQC spectra of RRM2/3 (black), RRM2 (red), and RRM3 (blue) in the absence of ligands is shown in Fig. S16a. Spectral overlay of RRM2 (residues 100–190) and RRM3 (residues 191–289) reproduced the spectrum of RRM2/3 (residues 100–289) well overall, although 35 pairs of corresponding signals did not overlap, which are labeled. Among the 35 pairs of signals, 9 and 26 pairs were from RRM2 and RRM3 residues, respectively (Fig. S16b). The 9 signals of RRM2 that did not overlap with the corresponding signals in RRM2/3 were in the C-terminal region (R172, E180, G184–F190), suggesting that the chemical shift differences were caused by the presence or absence of downstream RRM3.

In contrast, 26 signals of RRM3 did not overlap with the corresponding signals in RRM2/3 (T191, V193, Y194, K196, N197, L218, K221, V222, F235, V236, F238, R240, E242–A244, K246–E250, N252, V263, G264, A266, V270, E271). Mapping of these residues on the RRM3 structure indicated these they were near the N-terminus of RRM3 (Fig. S16c). In RRM2/3, the upstream sequence involved in RRM2 (residues 100–190) were directly attached to the N-terminus of RRM3, and isolated RRM3 possesses a cloning artifact sequence of GPLGS at its N-terminus. Therefore, the chemical shift differences of these signal pairs likely reflect the differences in the amino acid sequence at the N-terminus of RRM3.

Therefore, the spectral differences were not caused by the interaction between RRM2 and RRM3 in RRM2/3 but rather by differences in the sequence attached to C- and N-termini of RRM2 and RRM3, respectively.

## Supporting figures
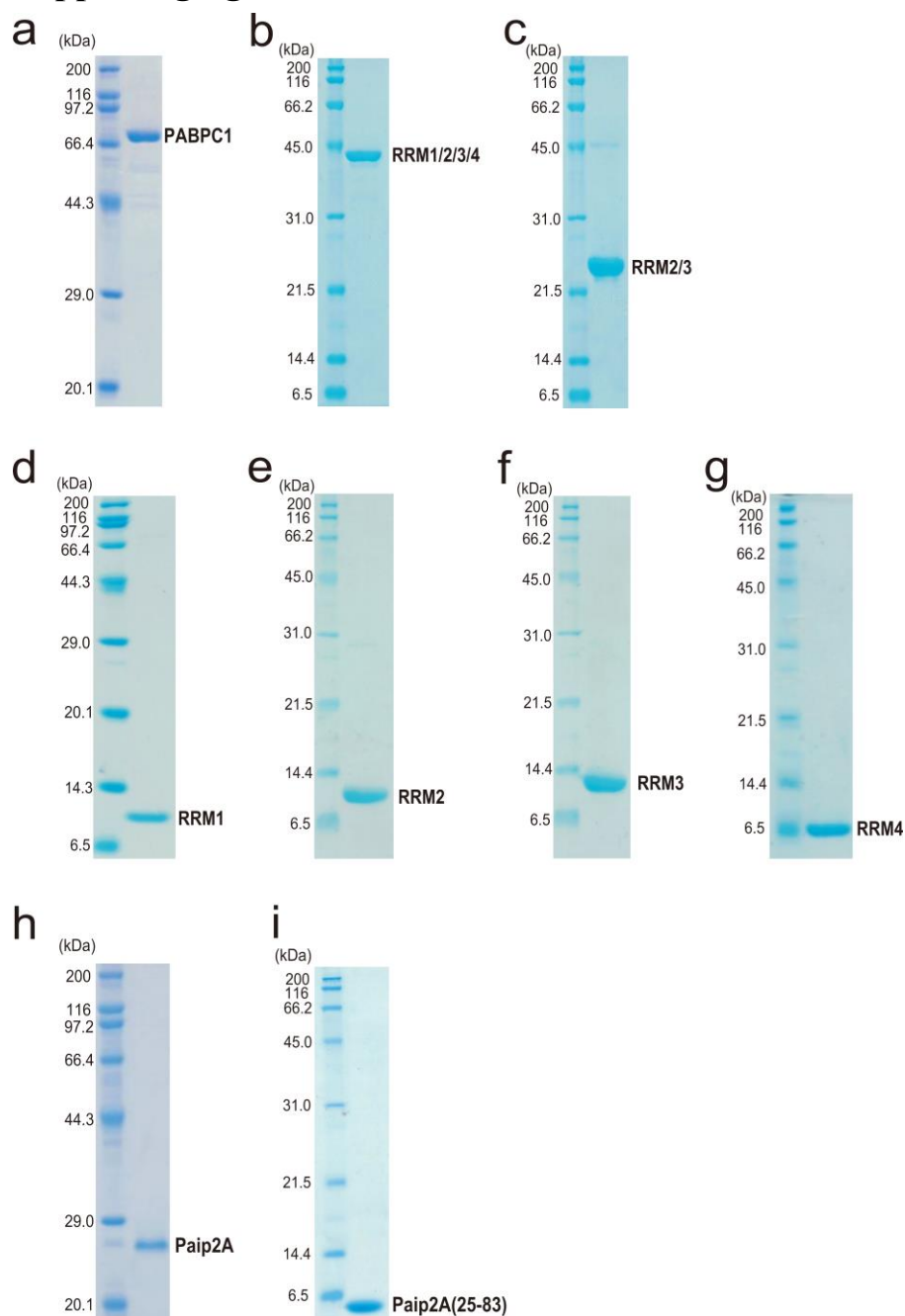


**Figure S1. Purity of prepared proteins**

SDS-PAGE analyses of prepared proteins: (a) PABPC1, (b) RRM1/2/3/4, (c) RRM2/3, (d) RRM1, (e) RRM2, (f) RRM3, (g) RRM4, (h) Paip2A, and (i) Paip2A(25–83). The band for Paip2A was observed at a molecular weight of 28 kDa, which is much higher than its theoretical molecular weight of 15 kDa. We confirmed that the molecular weight of the prepared Paip2A was 15 kDa using MALDI-TOF MS (data not shown).
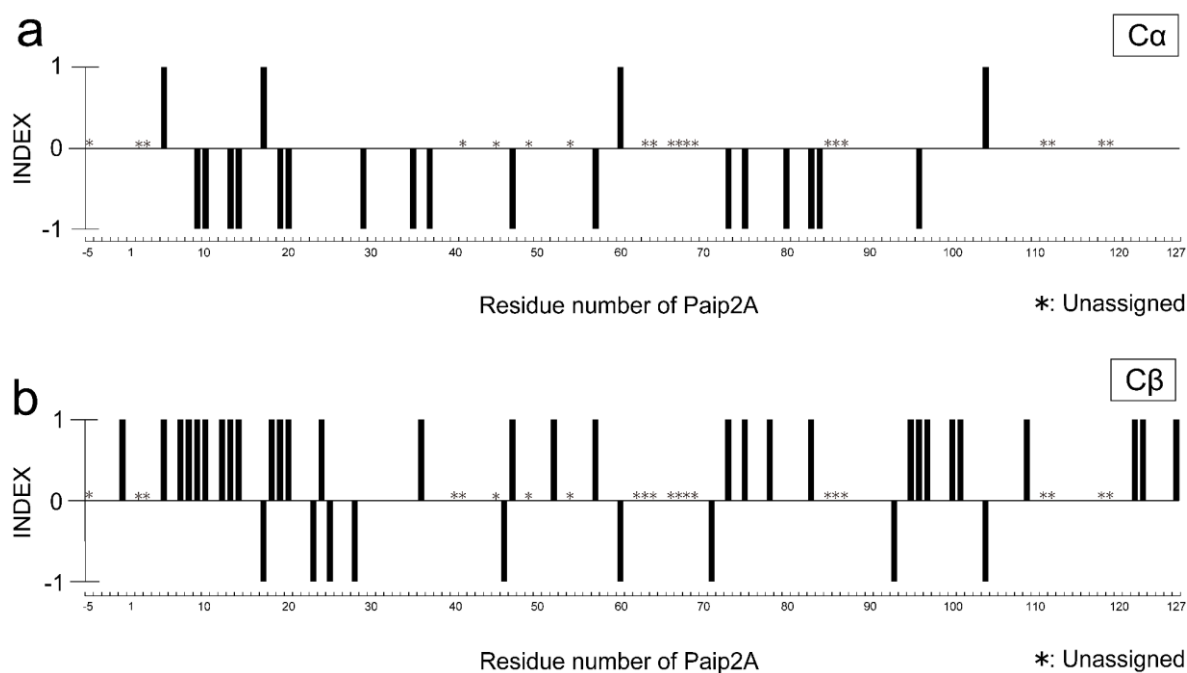
**Figure S2. Cα (a) and Cβ (b) chemical shift index of Paip2A(FL).**

The experiments were performed as described in the following paper: Wishart, D. S. and Sykes, B. D. (1994) The $^{13}$C Chemical-Shift Index: A simple method for the identification of protein secondary structure using $^{13}$C chemical-shift data. *J. Biomol*. *NMR* **4**, 171-180.

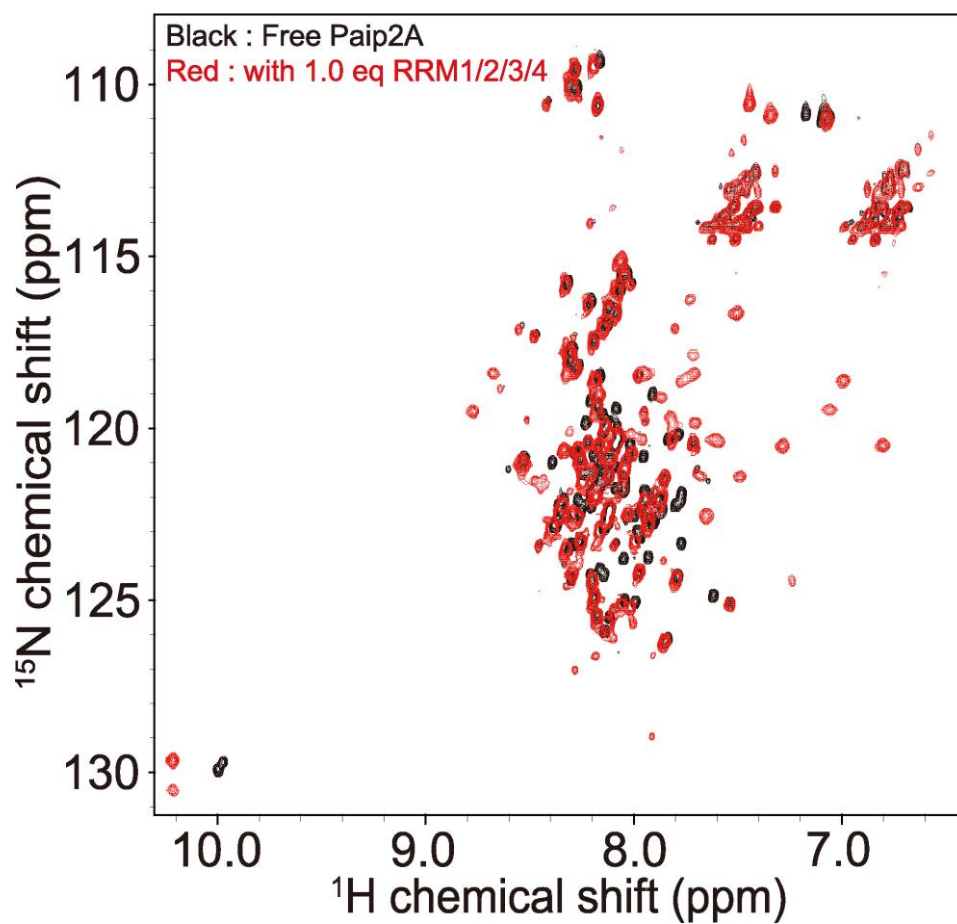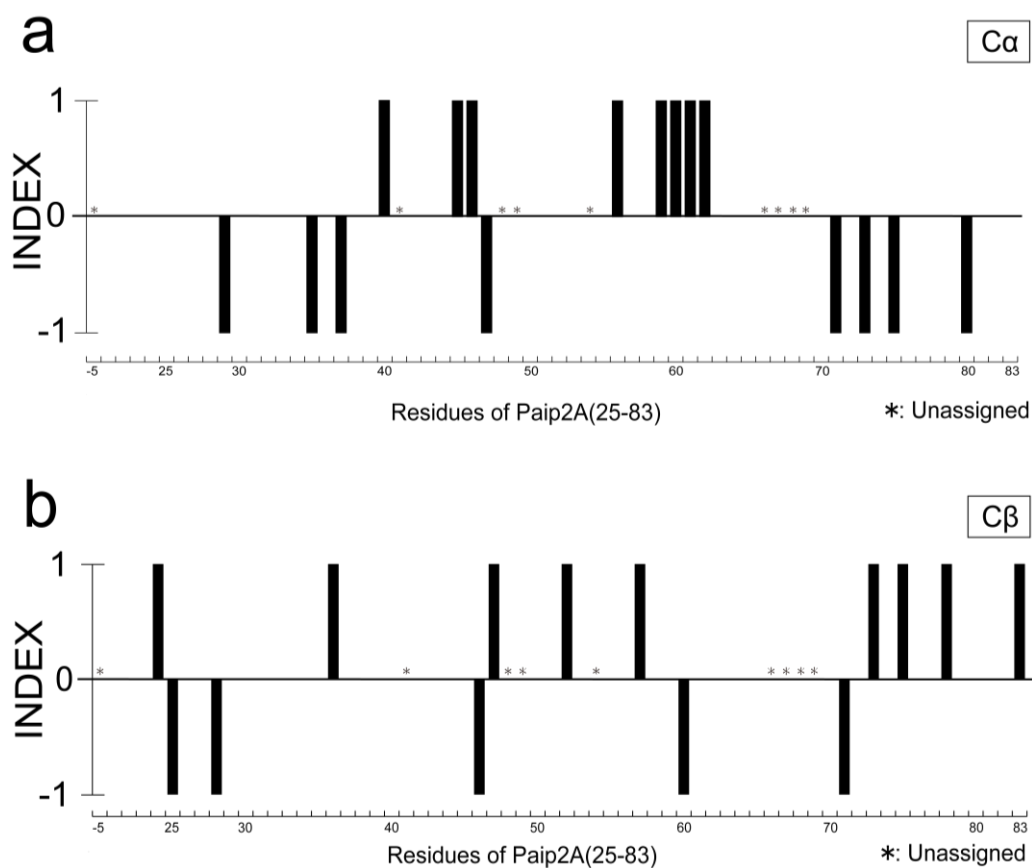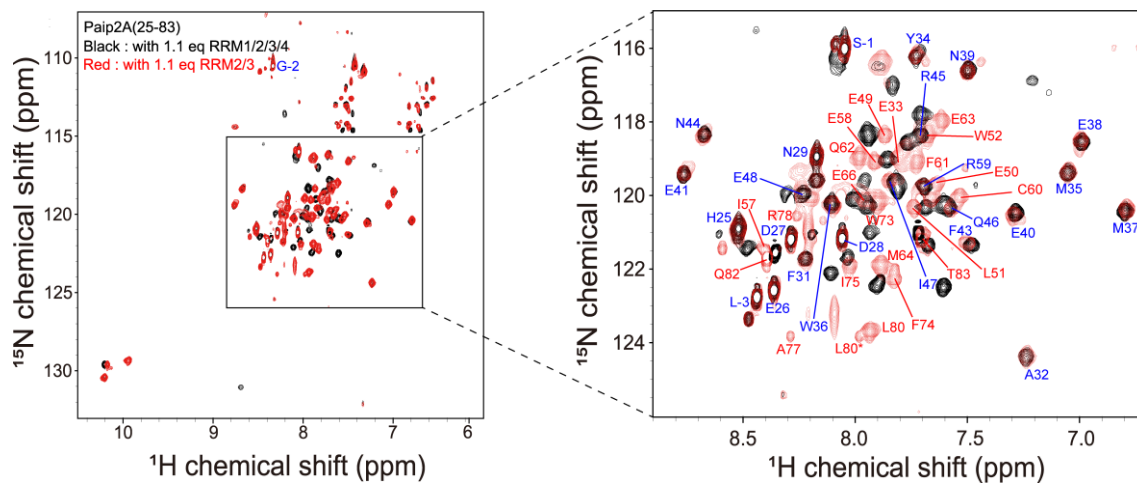**Figure S3. Overlay of full $^1$H-$^{15}$N TROSY spectra for $^2$H, $^{15}$N-labeled Paip2A(FL) in the presence (red) and absence (black) of non-labeled RRM1/2/3/4.**

**Figure S4. Cα (a) and Cβ (b) chemical shift index of Paip2A(25–83).**

The analyses were performed as described in the following paper: Wishart, D. S. and Sykes, B. D. (1994) The ^{13}C chemical-shift index: a simple method for the identification of protein secondary structure using ^{13}C chemical-shift data. *J. Biomol. NMR* **4**, 171-180.

**Figure S5. Overlay of $^{1}$H-$^{15}$N TROSY spectra of Paip2A(25-83) in the presence of RRM1/2/3/4 (black) and RRM2/3 (red)**
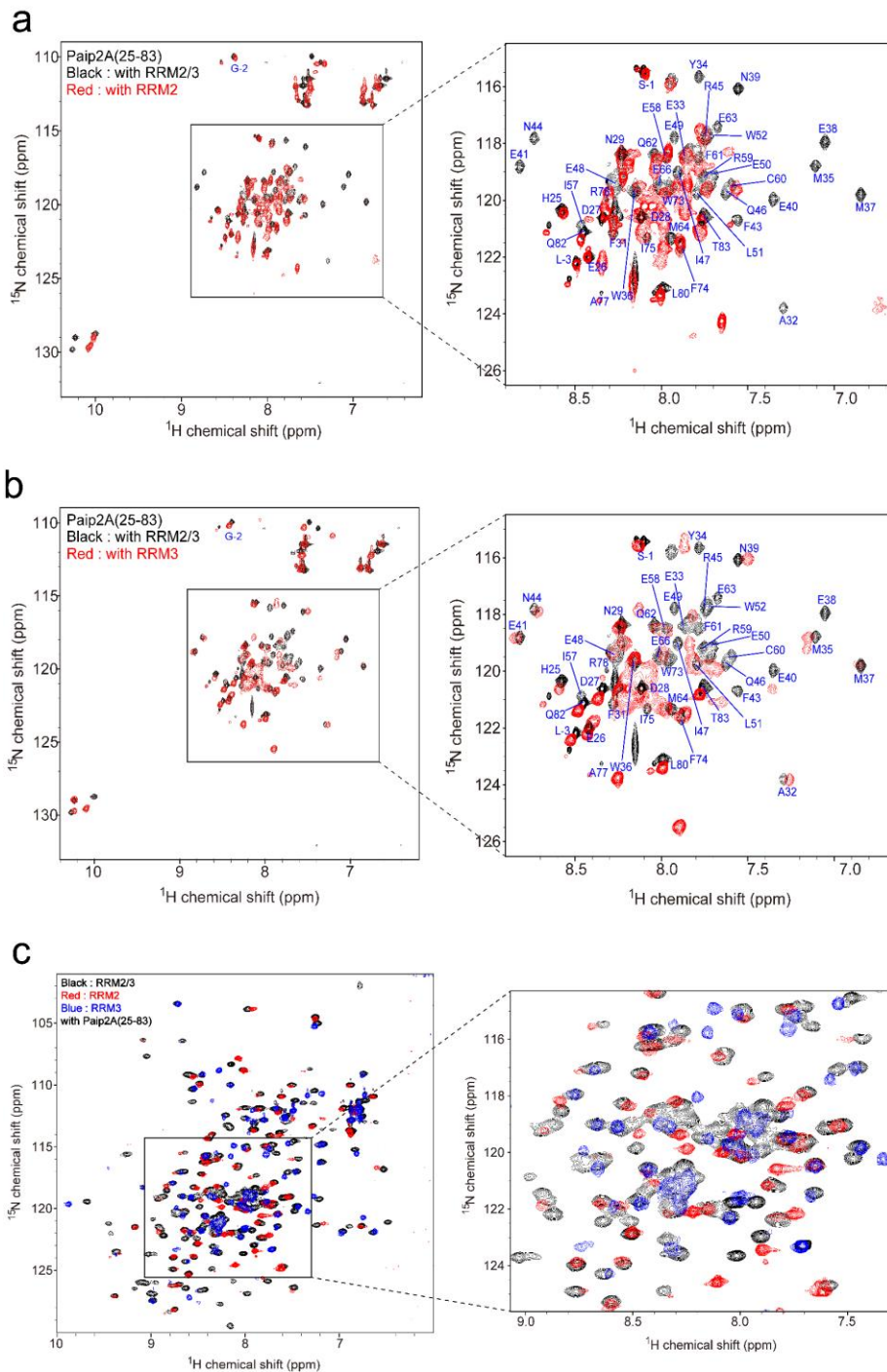
Signals that overlapped well between these two spectra are labeled as blue, whereas the remaining signals are labeled as red.
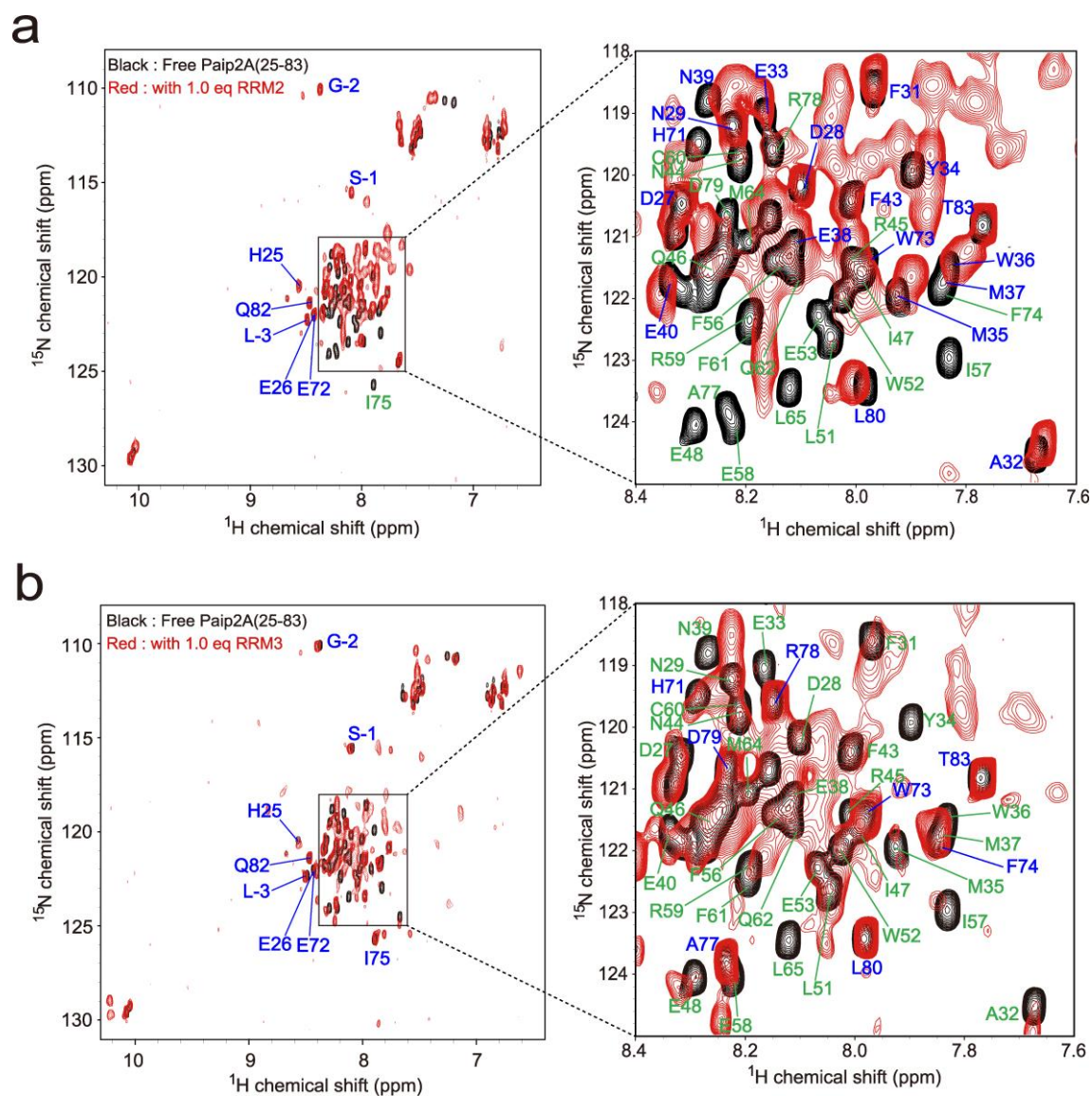
**Figure S6. (a) Overlay of $^{1}$H-$^{15}$N HSQC spectra of $^{15}$N-labeled Paip2A(25–83) in the absence (black) or presence (red) of RRM2 (a) and RRM3 (b).**

The perturbed and unperturbed signals are indicated in green and blue, respectively.

**Figure S7. Comparison of ¹H-¹⁵N HSQC spectra of ¹⁵N-labeled Paip2A(25–83) in complex with RRM2/3 and RRM2 or RRM3.**

Overlays of ¹H-¹⁵N HSQC spectra of Paip2A(25–83) in complex with RRM2/3 (black) or RRM2 (a) and RRM3 (b) (red). (c) Overlays of ¹H-¹⁵N HSQC spectra of RRM2/3 (black), RRM2 (red), and RRM3 (blue) in complex with Paip2A(25–83).
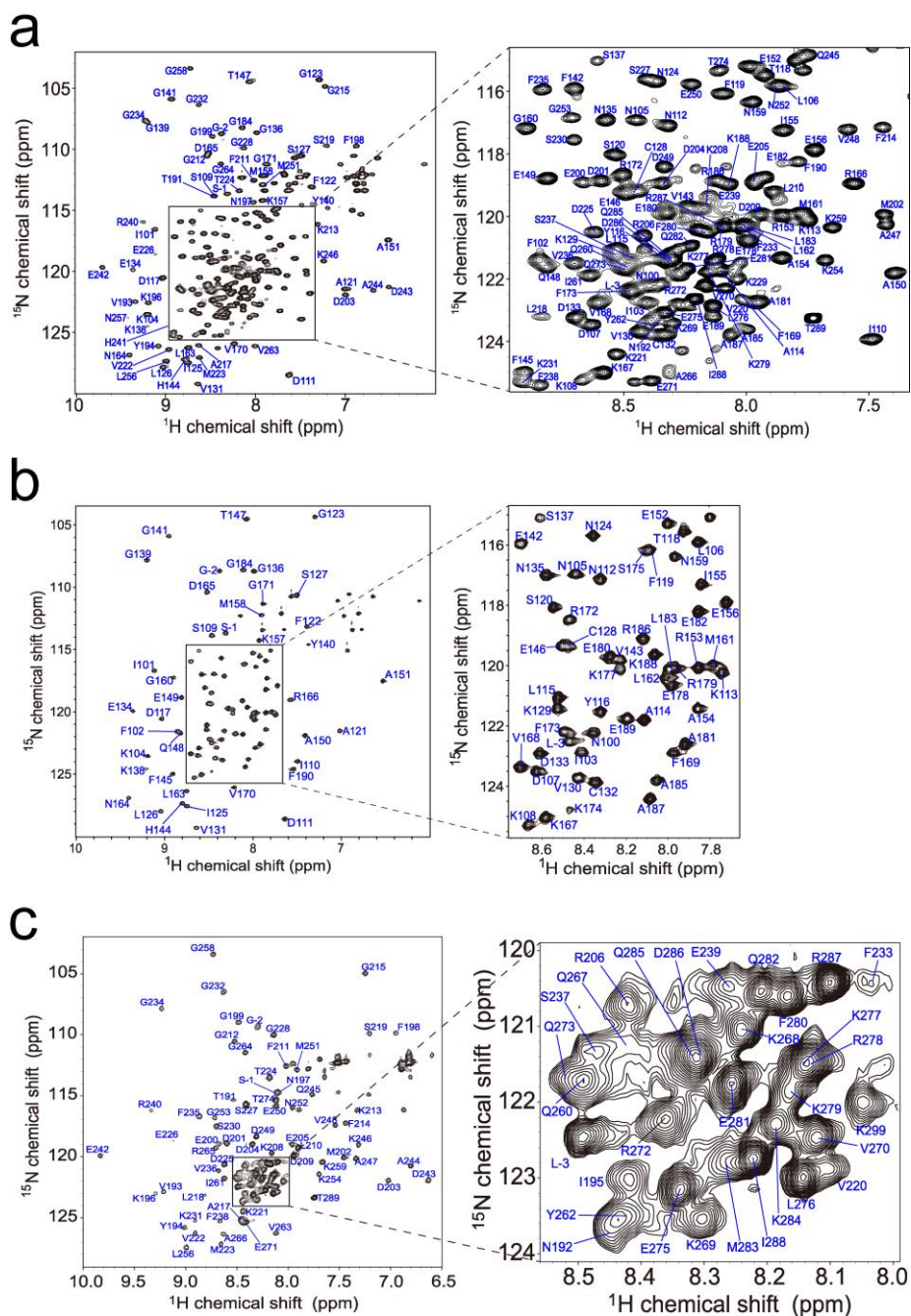
**Figure S8. Assignments of backbone amide signals on ¹H-¹⁵N HSQC spectra of RRM2/3, RRM2, and RRM3.**

Backbone amide signals in the ¹H-¹⁵N HSQC spectrum of (a) RRM2/3 were assigned using triple resonance spectra [HNCA and HN(CO)CA]. Those of (b) RRM2 and (c) RRM3 were assigned using triple resonance spectra [HNCACB, CBCA(CO)NH, and CCCONH], TOCSY, and NOESY spectra.
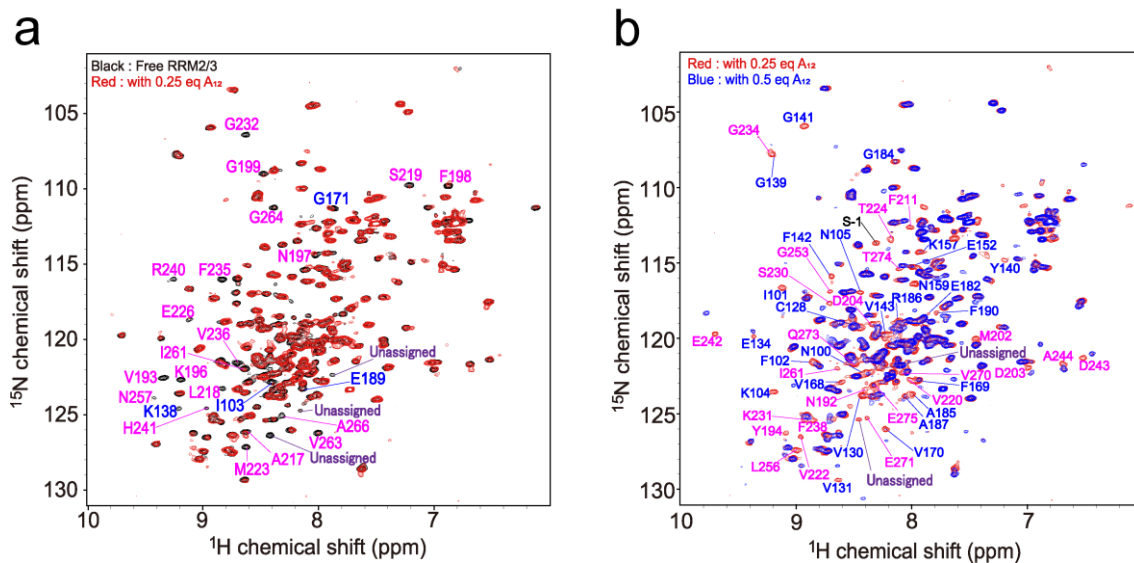
**Figure S9. NMR spectral changes during titrations showed different signals between RRM2 and RRM3 regions**

(a) Overlay of $^1$H-$^{15}$N HSQC spectra of $^{15}$N-labeled RRM2/3 in the absence (black) or presence (red) of 0.25 equivalents of $A_{12}$. Signals showing significantly reduced intensities and/or chemical shift changes after adding 0.25 equivalents of $A_{12}$ are labeled as blue (4) and magenta (20) for the RRM2 and RRM3 residues, respectively, and unassigned signals are labeled as "Unassigned" in purple. (b) Overlay of $^1$H-$^{15}$N HSQC spectra of $^{15}$N-labeled RRM2/3 in the presence of 0.25 equivalents of $A_{12}$ (red) and 0.5 equivalents of $A_{12}$ (blue). Signals showing significantly reduced intensities and/or chemical shift changes after adding 0.25–0.5 equivalents of $A_{12}$ are labeled as blue (26) and magenta (24) to identify residues of RRM2 and RRM3, respectively, and unassigned signals are labeled as "Unassigned" in purple.
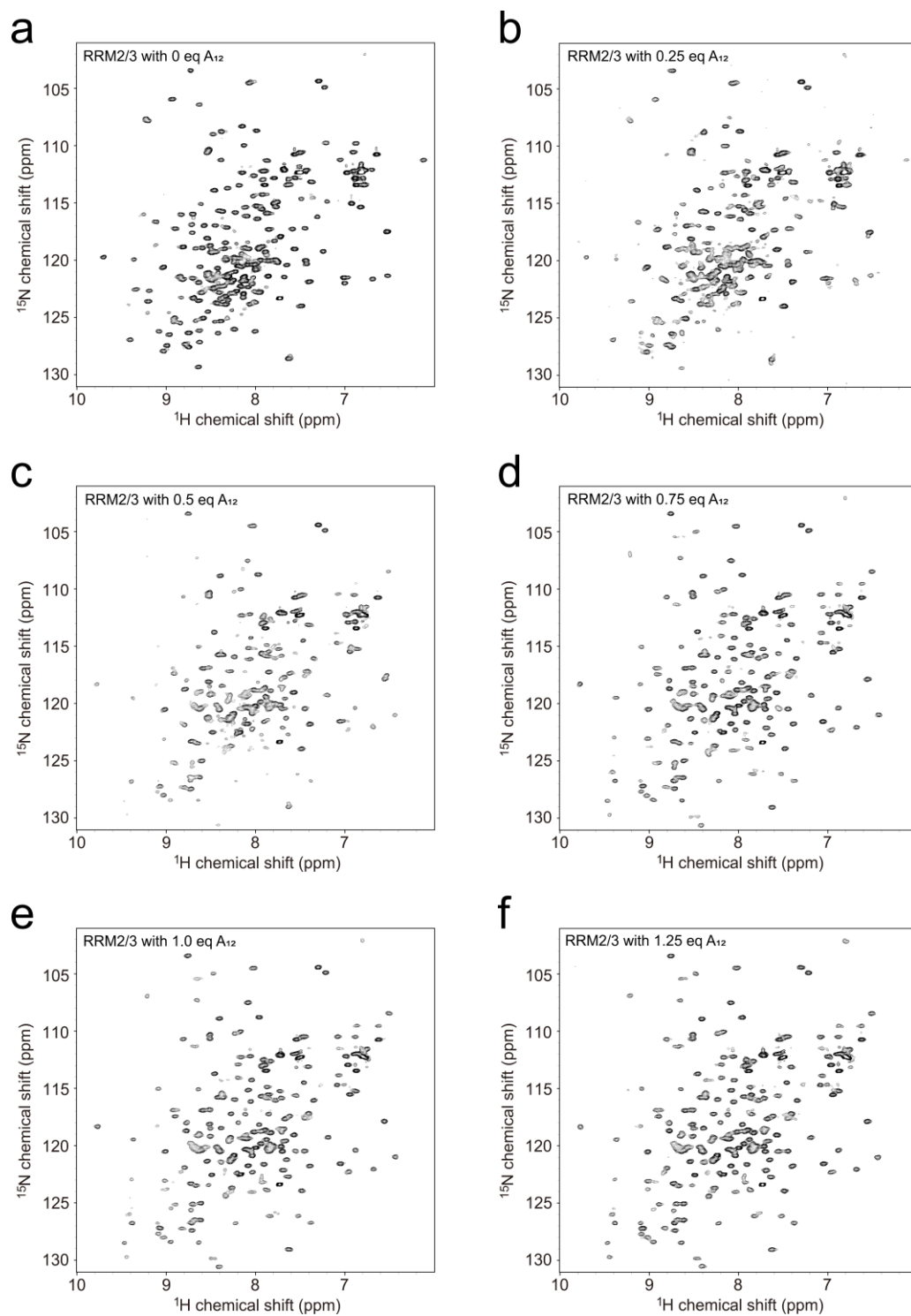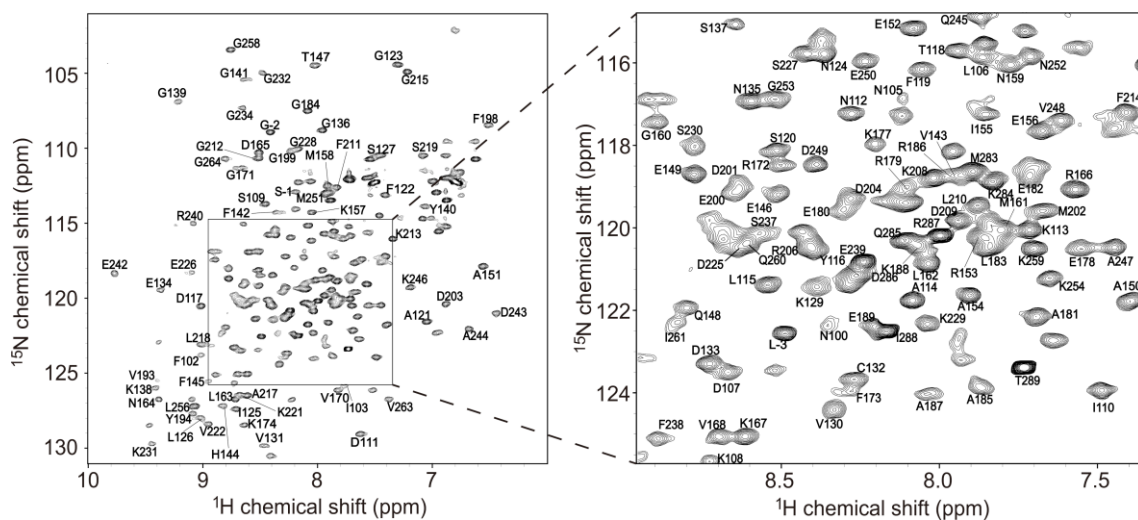
**Figure S10. $^1$H-$^{15}$N HSQC spectra of $^{15}$N-labeled RRM2/3 with titrations of A$_{12}$.**

A series of $^1$H-$^{15}$N HSQC spectra of $^{15}$N-labeled RRM2/3 in the absence (a) and presence of 0.25 (b), 0.5 (c), 0.75 (d), 1.0 (e), and 1.25 (f) equivalents of A$_{12}$.
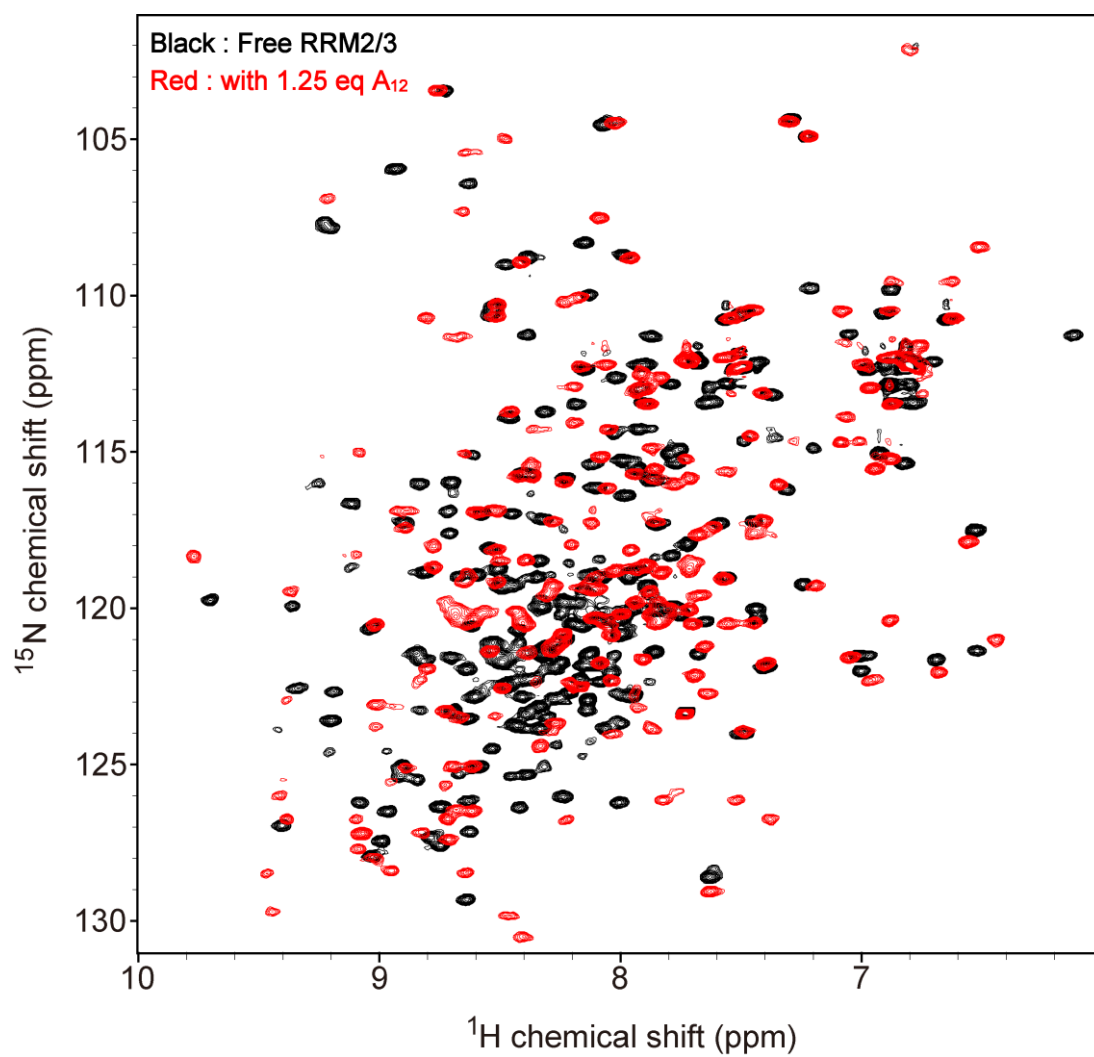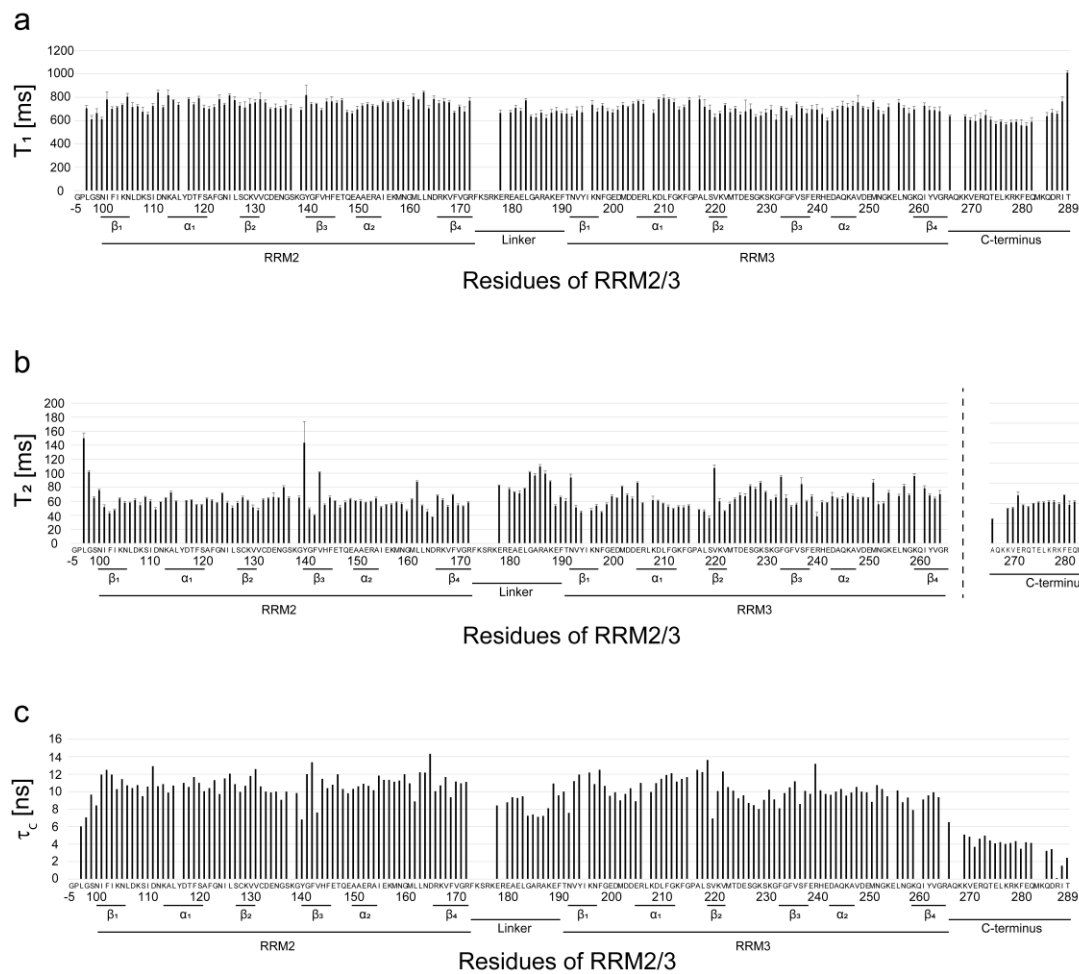
**Figure S11. Overlay of $^1$H-$^{15}$N HSQC spectra of RRM2/3 in the free state (black) and in the presence of 1.25 equivalents of A$_{12}$ (red).**

**Figure S12. Assignments of backbone amide signals on $^1$H-$^{15}$N HSQC spectra of A$_{12}$-bound RRM2/3.**

Backbone NMR assignments of A$_{12}$-bound RRM2/3 are indicated in the $^1$H-$^{15}$N HSQC spectrum. We assigned 152 (80%) backbone NMR resonances for RRM2/3 among the 189 theoretically observable resonances by analyzing several triple resonance experiments using the uniformly $^{13}$C, $^{15}$N-labeled RRM2/3-A$_{12}$ complex, and the results of RRM2-A$_7$ and RRM3-A$_7$ titrations.
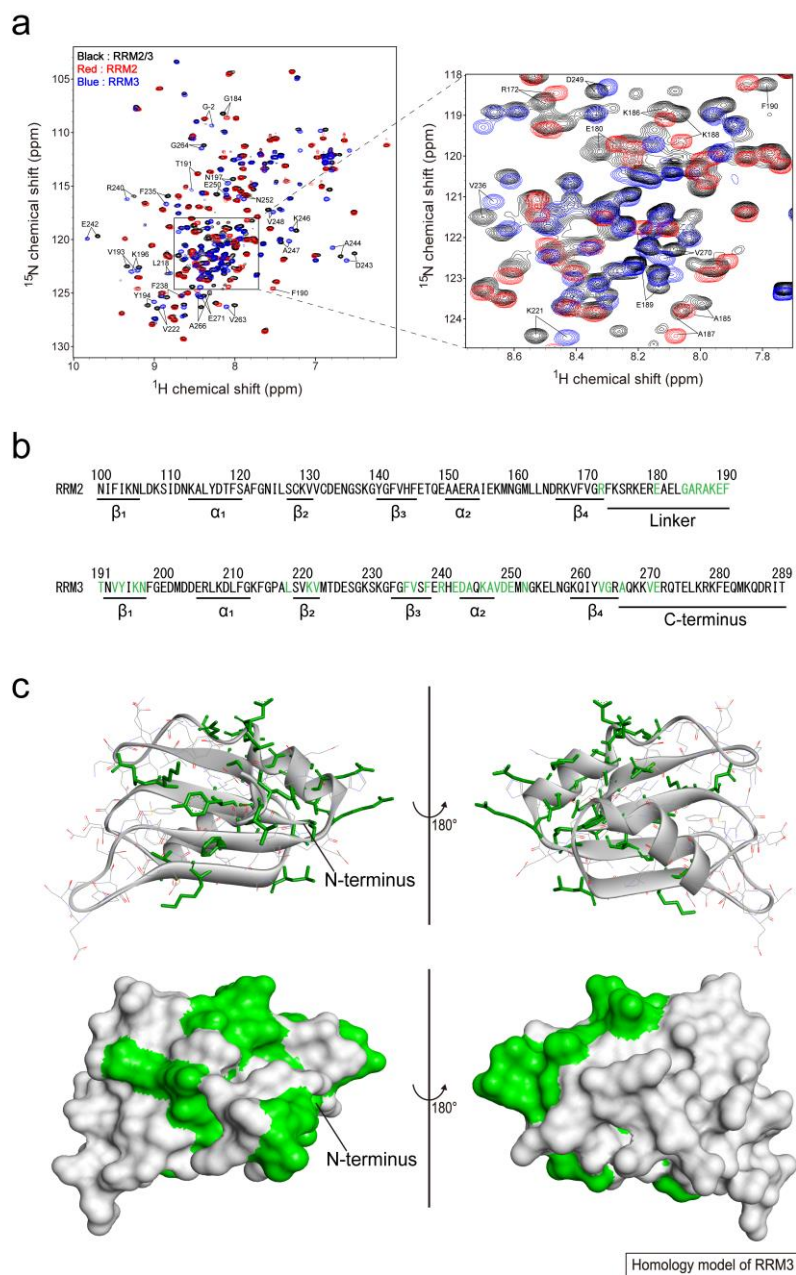
**Figure S13. Graphs of $T_1$ (a), $T_2$ (b), and $\tau_c$ (c) versus each residue of RRM2/3.**
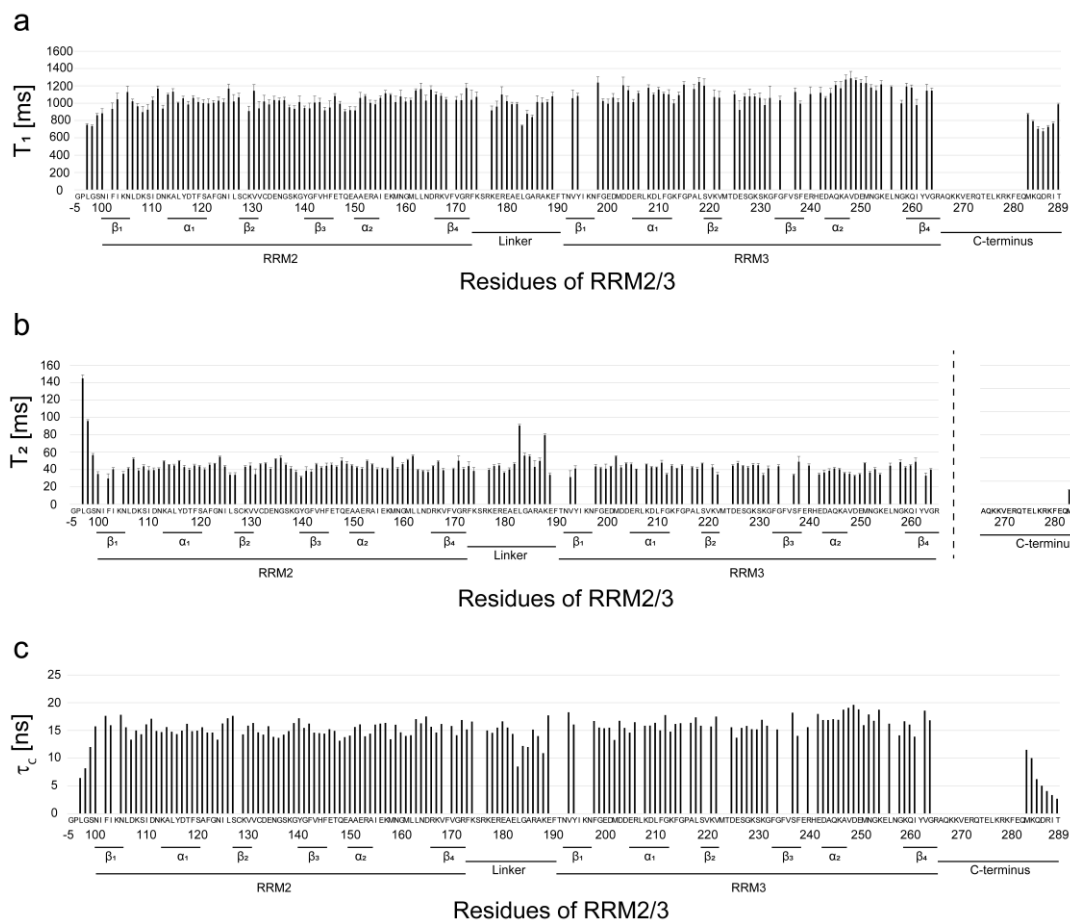
**Figure S14. Graphs of** $T_1$ **(a),** $T_2$ **(b), and** $\tau_c$ **(c) versus each residue of RRM2/3 bound to A$_{12}$.**

**Figure S15. Comparison of ¹H-¹⁵N HSQC spectra of ¹⁵N-labeled RRM2/3, RRM2 and RRM3 in the free state**

(a) Overlay of ¹H-¹⁵N HSQC spectra of RRM2/3 (black), RRM2 (red) and RRM3 (blue). The signals that do not overlap between the tandem RRM2/3 domain and isolated RRM2 or RRM3 are labeled. (b) Residues with signals that do not overlap in (a) are colored as green. (c) Labeled residues of RRM3 in (b) are mapped on the structure of RRM3.
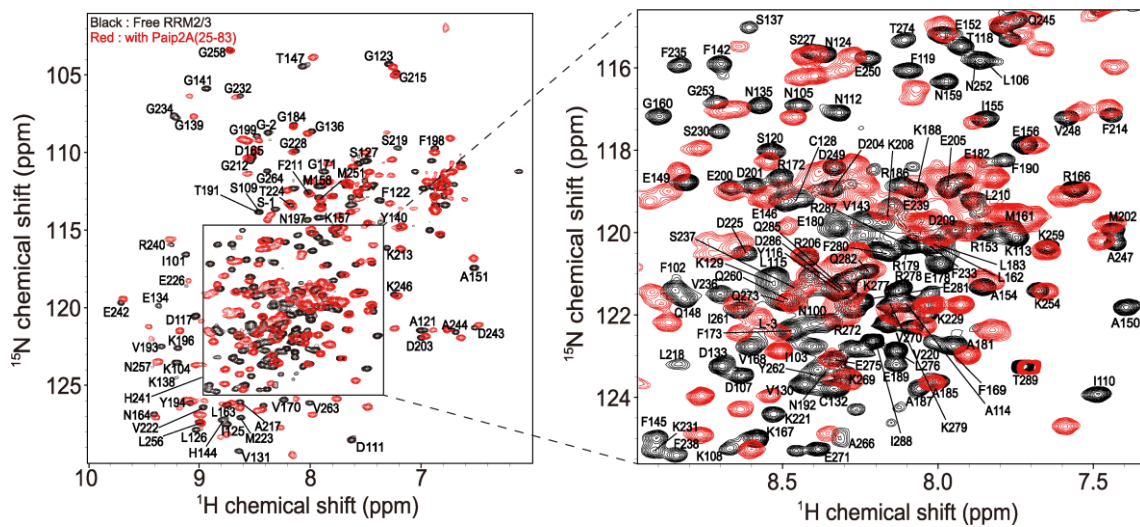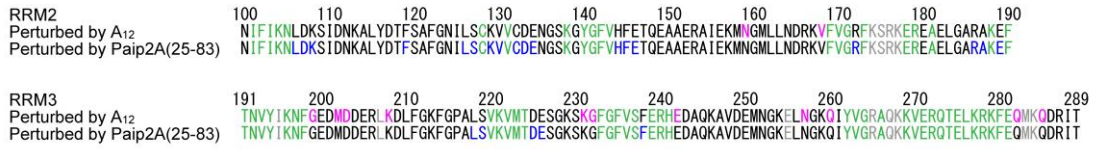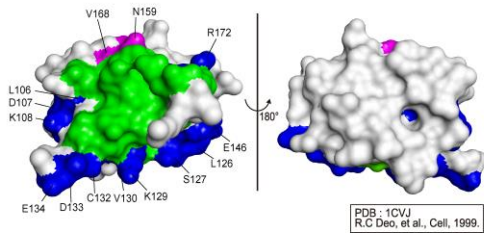
**Figure S16. Overlay of full $^1$H-$^{15}$N HSQC spectra of $^{15}$N-labeled RRM2/3 in the absence (black) and presence (red) of 1.25 equivalents of Paip2A(25–83).**
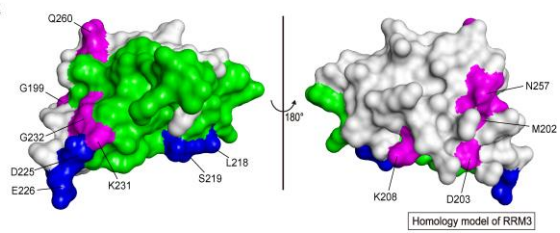
**Figure S17. Comparison of RRM2/3 residues involved in $A_{12}$ and Paip2A(25–83) binding, and mapping of these residues onto the structures of RRM2 and RRM3.**

(a) Comparison of RRM2/3 residues involved in $A_{12}$ and Paip2A(25–83). Residues showing chemical shift changes of more than 0.2 ppm in Fig. 7d are colored as magenta, residues labeled as "perturbed" in Fig. 8c are colored as blue, and residues perturbed by both $A_{12}$ and Paip2A(25–83) are colored as green.

(b) Mapping of $A_{12}$-interacting and Paip2A(25–83)-interacting residues onto the structure of RRM2, and (c) those of RRM3. Residues perturbed by both $A_{12}$ and Paip2A(25–83) are colored as green, perturbed by $A_{12}$ only were colored as magenta, and perturbed by Paip2A(25–83) only were colored as blue.
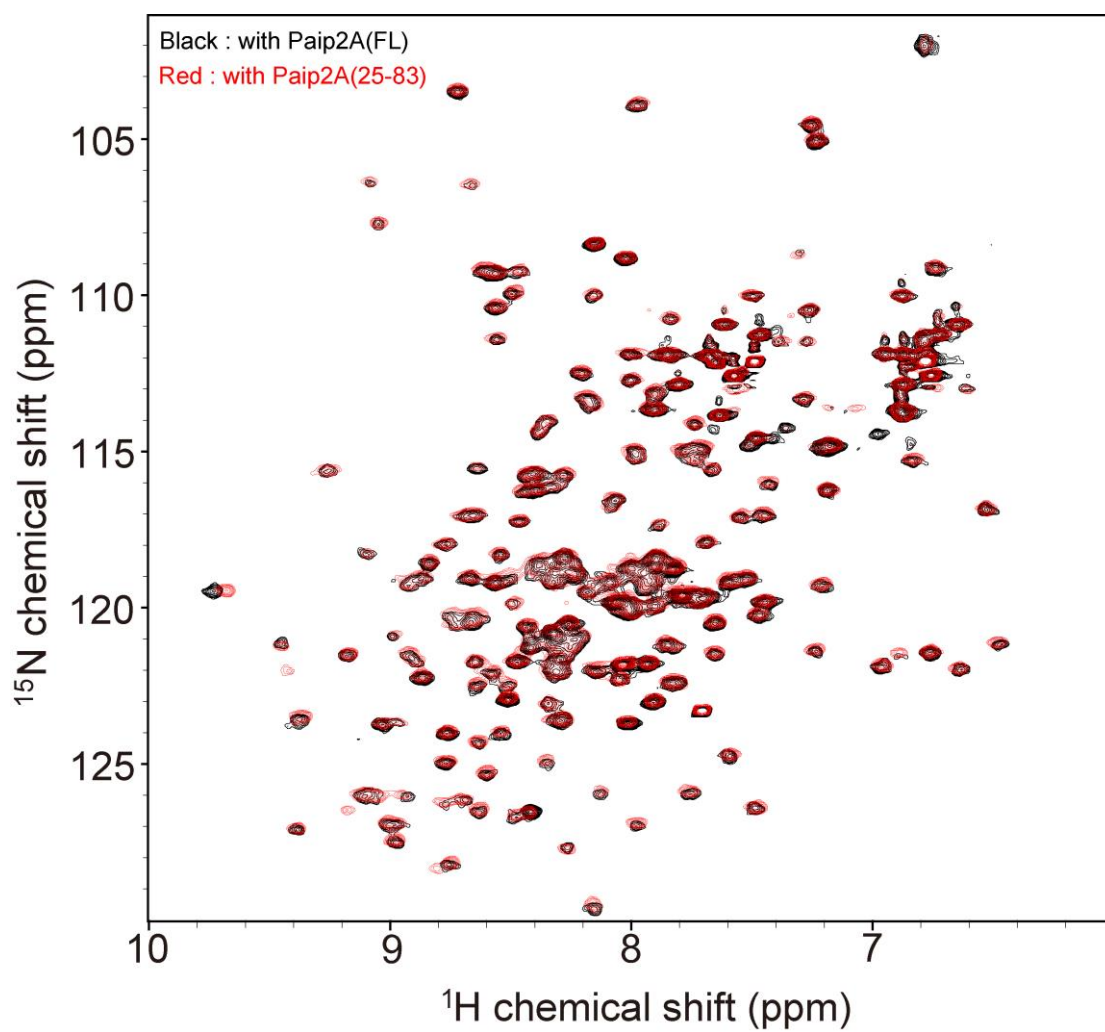
**Figure S18. Comparison of $^1$H-$^{15}$N HSQC spectra of RRM2/3 in the presence of Paip2A(FL) (black) and Paip2A(25–83) (red).**

```
RRM     Residue number  Sequence
RRM1    1-99            MNPSAPSYPMASLYVGDLHPDVTEAMLYEKFSPAGPILSIRVCRDMITRRSLGYAYVNFQQPADAERALDTMNFDVIKGKPVRIMWSQRDPSLRKSGVG------------
RRM2    100-190         -----------NIFIKNLDKSIDNKALYDTFSAFGNILSCKVVCDE-NG-SKGYGFVHFETQEAAERAIEKMNGMLLNDRKVFVGRFKSRKER-EAELGARAKEF------
RRM3    191-289         -----------TNVYIKNFGEDMDDERLKDLFGKFGPALSVKVMTDE-SGKSKGFGFVSFERHEDAQKAVDEMNGKELNGKQIYVGRAQKKVER-QTELKRKFEQMKQDRIT
RRM4    290-371         -------RYQGVNLYVKNLDDGIDDERLRKEFSPFGTITSAKVMM-E-GGRSKGFGFVCFSSPEEATKAVTEMNGRIVATKPLYVALAQRK--------------------
                        .::: ::  .: :  *. *.  *   * :*      * *:.:* *.   * :*: **   :  :  : :  :
```

"*" : Conserved in all domains
" : " : Amino acids have the same properties.
" . " : Amino acids have similar properties.

**Figure S19. Sequence alignment of each RRM domain**

Sequence alignment was performed using Clustal Omega. The sequences of RRM1, RRM2, RRM3, and RRM4 are residue numbers 1–99, 100–190, 191–289, and 290–371 of PABPC1, respectively.

# Supporting tables

**Table S1. Mean values of $T_1$, $T_2$, and $\tau_c$ for each region of RRM2/3.**

RRM2 consists of residues 100–172 of PABPC1, the linker between RRM2 and RRM3 consists of residues 173–190 of PABPC1, RRM3 consist of residues 191–265 of PABPC1, and the C-terminus of RRM2/3 consists of residues 266–289.

| Region | $T_1$ [ms] | $T_2$ [ms] | $\tau_c$ [ns] |
|--------|-----------|------------|---------------|
| RRM2   | 740 ± 45  | 60.5 ± 14.0 | 10.8 ± 1.2 |
| Linker | 672 ± 39  | 83.0 ± 15.8 | 8.6 ± 1.2  |
| RRM3   | 700 ± 42  | 64.4 ± 14.0 | 10.2 ± 1.2 |

$T_1$: spin-lattice relaxation time

$T_2$: spin-spin relaxation time

$\tau_c$: rotational correlation time

**Table S2. Mean values of $T_1$, $T_2$, and $\tau_c$ for each region of RRM2/3 in complex with $A_{12}$.**
RRM2 consists of residues 100–172 of PABPC1, the linker between RRM2 and RRM3 consists of residues 173–190 of PABPC1, RRM3 consist of residues 191–265 of PABPC1, and the C-terminus of RRM2/3 consists of residues 266–289.

| Region | $T_1$ [ms] | $T_2$ [ms] | $\tau_c$ [ns] |
|--------|-----------|-----------|---------------|
| RRM2   | 1024 ± 74 | 43.2 ± 5.5 | 15.3 ± 1.2 |
| Linker | 977 ± 94  | 49.5 ± 15.3 | 14.3 ± 2.3 |
| RRM3   | 1118 ± 71 | 41.6 ± 5.5 | 16.3 ± 1.2 |

$T_1$: spin-lattice relaxation time

$T_2$: spin-spin relaxation time

$\tau_c$: rotational correlation time